MNRAS **000**, 1–14 (2018) Preprint 18 May 2022 Compiled using MNRAS LATEX style file v3.0

Massive Neutrinos Leave Fingerprints on Cosmic Voids

C. D. Kreisch[1⋆], A. Pisani [1,2]†, C. Carbone[3,4], J. Liu [1], A. J. Hawken[2], E. Massara[5,6], D. N. Spergel[1,6] , B. D. Wandelt [1,6,7,8]

[1] *Princeton University, Princeton, NJ 08544 USA*
[2] *Aix-Marseille Université, CNRS/IN2P3, CPPM, Marseille, France*
[3] *Università degli studi di Milano-Dipartimento di Fisica, via Celoria, 16, 20133 Milano, Italy*
[4] *INAF-Osservatorio Astronomico di Brera, Via Brera, 28, 20121 Milano, Italy*
[5] *Berkeley Center for Cosmological Physics, University of California, Berkeley, CA 94720 USA*
[6] *Center for Computational Astrophysics, Flatiron Institute, 162 5th Avenue, New York, NY 10010 USA*
[7] *Institut d'Astrophysique de Paris, 98bis Boulevard Arago, 75014 Paris, France*
[8] *Sorbonne Universités, Institut Lagrange de Paris, 98 bis Boulevard Arago, 75014 Paris, France*

arXiv:1808.07464v1 [astro-ph.CO] 22 Aug 2018

18 May 2022

ABSTRACT

Massive neutrinos uniquely affect cosmic voids. We explore their impact on void clustering using both the `DEMNUni` and `MassiveNuS` simulations. For voids, neutrino effects depend on the observed void tracers. As the neutrino mass increases, the number of small voids traced by cold dark matter particles increases and the number of large voids decreases. Surprisingly, when massive, highly biased, halos are used as tracers, we find the opposite effect. How neutrinos impact the scale at which voids cluster and the void correlation is similarly sensitive to the tracers. This scale dependent trend is not due to simulation volume or halo density. The interplay of these signatures in the void abundance and clustering leaves a distinct fingerprint that could be detected with observations and potentially help break degeneracies between different cosmological parameters. This paper paves the way to exploit cosmic voids in future surveys to constrain the mass of neutrinos.

Key words: large scale structure of universe – Cosmology: theory – cosmological parameters

1 INTRODUCTION

The cosmic web (Bond et al. 1996) is a powerful tool to constrain neutrino properties. Cosmic voids are large (typically $10-100\,h^{-1}$Mpc) underdense regions of the cosmic web that have undergone minimal virialization and are dominated by inward or outward bulk flows (Shandarin 2011; Falck & Neyrinck 2015; Ramachandra & Shandarin 2017). In contrast to halos, which have undergone non-linear growth that can wash out primordial information, voids offer a pristine environment to study cosmology. As such, voids are a complementary probe to measurements of the cosmic microwave background and galaxy clustering and can help break existing degeneracies between cosmological parameters, thus becoming increasingly popular to study with both simulations and observations (see e.g. Ryden 1995; Goldberg & Vogeley 2004; Colberg et al. 2008; Viel et al. 2008; Van De Weygaert & Platen 2011; Paranjape et al. 2012; Chan et al. 2014; Hamaus et al. 2014b; Sutter et al. 2014b,c; Hamaus et al. 2015; Szapudi et al. 2015; Qin et al. 2017; Alonso et al. 2018; Pollina et al. 2018, and references therein).

The discovery of neutrino oscillations demonstrate that at least two neutrino families must have a nonzero mass (Becker-Szendy et al. 1992; Fukuda et al. 1998; Ahmed et al. 2004), evidence for beyond the standard model physics. Cosmological observables provide stringent upper bounds on the sum of neutrino masses, Σm_ν (see e.g. Planck Collaboration et al. 2018), and may soon determine the last missing parameter in the standard model.

At linear order, neutrinos do not cluster on scales smaller than their free-streaming length, which is a function of the mass m_ν of the single neutrino species (Lesgourgues & Pastor 2006). For example, neutrinos have free-streaming lengths of $130\,h^{-1}$Mpc and $39\,h^{-1}$Mpc for $\Sigma m_\nu = 0.06\,$eV and $\Sigma m_\nu = 0.6\,$eV (assuming 3 degenerate neutrino species), respectively. Neutrino free-streaming scales for Σm_ν of interest thus fall within the range of typical void sizes, making voids an interesting tool for studying neutrinos.

Voids are sensitive to a number of effects, such as: redshift space distortions and the relative growth rate of cosmic structure (e.g. Paz et al. 2013; Hamaus et al. 2016; Achitouv

⋆ E-mail: ckreisch@astro.princeton.edu
† E-mail: apisani@astro.princeton.edu

© 2018 The Authors

et al. 2016; Hamaus et al. 2017; Hawken et al. 2016), Alcock-Paczyński distortions (e.g. Alcock & Paczyński 1979; Lavaux & Wandelt 2012; Sutter et al. 2012, 2014d; Hamaus et al. 2014c, 2016; Mao et al. 2017; Achitouv & Cai 2018), weak gravitational lensing (e.g. Melchior et al. 2013; Clampitt & Jain 2015; Clampitt et al. 2017; Chantavat et al. 2017), baryon acoustic oscillations (Kitaura et al. 2016), and the integrated Sachs-Wolfe effect (e.g. Granett et al. 2008; Ilić et al. 2013; Kovács & Granett 2015; Kovács & García-Bellido 2016; Nadathur & Crittenden 2016; Naidoo et al. 2016; Cai et al. 2017; Kovács et al. 2017).

Voids offer an environment with unique sensitivity to signatures of physics beyond the standard model. They are one of the best observables to probe theories of gravity (Odrzywołek 2009; Li et al. 2012; Clampitt et al. 2013; Cai et al. 2014; Gibbons et al. 2014; Zivick & Sutter 2014; Barreira et al. 2015; Hamaus et al. 2016; Baldi & Villaescusa-Navarro 2018) and dark energy (Lee & Park 2009; Bos et al. 2012; Lavaux & Wandelt 2012; Sutter et al. 2014e; Pisani et al. 2015; Pollina et al. 2016).

Since voids are under-dense in matter, they are particularly sensitive to the effects of diffuse components in the universe like radiation and dark energy. For this reason, voids offer an appealing, new avenue to constrain neutrino properties. Villaescusa-Navarro et al. (2013) studied how massive neutrinos affect voids at high redshifts with Lyα forest analyses using hydrodynamical simulations (see also Krolewski et al. 2017). Massara et al. (2015) focused on how neutrinos affect void abundance, density profiles, ellipticities, the correlation function, and velocity profiles with N-body simulations that included massive neutrinos as an additional collisionless particle component. Banerjee & Dalal (2016) observed that neutrinos affect the scale-dependent void bias for voids traced by the CDM particle field. They use a spherical void finder and a small volume simulation (700 h^{-1}Mpc box length). In recent data analyses voids have been found using finders that do not assume spherical voids (e.g. Hamaus et al. 2017; Pollina et al. 2017). It is interesting to analyze the effects of neutrinos on voids with non-spherical shapes, such as in Massara et al. (2015), which have advantage of closely following the cosmic web pattern. Work such as Hamaus et al. (2014a) analyzed void power spectra without discussion of neutrinos. Thus far, the effect of neutrinos on voids has not been considered in depth without assuming spherical voids, and their effect on voids traced by halos is especially unexplored. Previous simulations with massive neutrinos did not have the volume and resolution to explore the effect of neutrinos on voids derived from the halo distribution and Halo Occupation Distribution (HOD) mocks (see e.g. Massara et al. 2015).

For the first time, we use N-body simulations with densities and volumes large enough to distinguish the effects neutrinos have on voids derived from the halo distribution and on voids derived from the particle distribution. The paper is organized as follows. In §2 we describe the two sets of massive neutrino simulations used in this work, the Dark Energy and Massive Neutrino Universe Project (`DEMNUni`) and the Cosmological Massive Neutrino Simulations (`MassiveNuS`), as well as the void finder used to build our void catalog. We show how neutrinos impact voids in §3 and discuss these results in §4. We conclude and discuss application to future surveys in §5.

2 SIMULATIONS AND VOID FINDER

In this work, we use two sets of massive neutrino simulations: the Dark Energy and Massive Neutrino Universe (`DEMNUni`, Carbone et al. 2016; Castorina et al. 2015), and the Cosmological Massive Neutrino Simulations (`MassiveNuS`[1], Liu et al. 2018). We isolate the effects of Σm_ν by comparing the large volume DEMNUni simulations (2 h^{-1}Gpc box length, 2048^3 CDM particles plus 2048^3 ν particles) with the smaller but more highly resolved `MassiveNuS` simulations (512 h^{-1}Mpc box length, 1024^3 CDM particles– i.e. eight times higher resolution than `DEMNUni` but 60 times smaller in volume). We focus our analysis on the simulation snapshots at $z = 0$.

Comparing how neutrinos affect voids for different tracers is imperative when looking towards constraining the sum of neutrino masses with upcoming surveys. Surveys observe galaxies, which are biased tracers of the CDM fluctuations (Villaescusa-Navarro et al. 2014; Castorina et al. 2014), and void properties are sensitive to the tracer used to build the void catalog (Pollina et al. 2016, 2017). We rely on the optimal features of both simulations to be sensitive to neutrino effects at different scales, show consistency, check that our results are physical, and robustly test the sensitivity of our results to simulation design (see Appendix B for volume and resolution tests). The small volume and high resolution of `MassiveNuS` causes these simulations to be dominated by small voids, capturing the small scale impacts of Σm_ν, whereas the large volume of the `DEMNUni` simulations captures large scale effects. `MassiveNuS`'s high resolution enables the use of halos above a minimum mass $M_{\rm min} = 3 \times 10^{11}\, h^{-1} M_\odot$ whereas `DEMNUni`'s minimum halo mass is $M_{\rm min} = 2.5 \times 10^{12}\, h^{-1} M_\odot$, making `MassiveNuS` halos less biased than `DEMNUni`. The two simulations also use different methods to capture the effect of massive neutrinos– `DEMNUni` neutrinos are treated as particles and `MassiveNuS` neutrinos use a fast linear response algorithm (Ali-Haïmoud & Bird 2013).

The sum of neutrino masses Σm_ν is varied in each simulation suite with other cosmological parameters kept fixed. The `DEMNUni` simulations assume a baseline cosmology according to the Planck results (Planck Collaboration et al. 2013), with $h = 0.67$, $n_s = 0.96$, $A_s = 2.1265 \times 10^{-9}$, $\Omega_m = 0.32$, and $\Omega_b = 0.05$. The relative energy densities of cold dark matter Ω_c (and neutrinos, Ω_ν) vary for each model as $\Omega_c = 0.27$, 0.2659, 0.2628 and 0.2573, for $\Sigma m_\nu = 0$, 0.17, 0.30 and 0.53 eV, respectively. In the considered cases, since A_s is fixed while varying the neutrino mass, the simulations with massive neutrinos have a lower value of σ_8 with respect to the massless neutrino ΛCDM case. We use the three fiducial models of `MassiveNuS` in this work, where $\Sigma m_\nu = 0$, 0.1, 0.6 eV and all other parameters are held constant at A_s=2.1×10^{-9}, Ω_m=0.3, h=0.7, n_s=0.97, w=−1, and Ω_b=0.05.

We use the public void finder `VIDE`[2] to locate voids in the simulations (Sutter et al. 2015). Because the void finder

[1] The `MassiveNuS` data products, including snapshots, halo catalogues, merger trees, and galaxy and CMB lensing convergence maps, are publicly available at `http://ColumbiaLensing.org`.
[2] `https://bitbucket.org/cosmicvoids/vide_public`, version most recently updated on 2017 – 11 – 27.

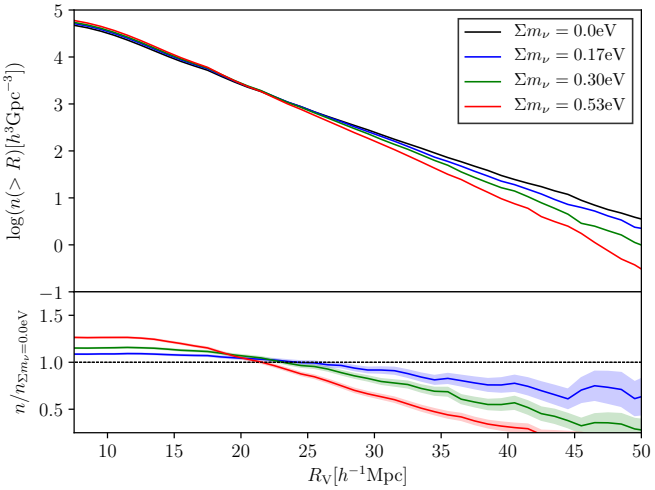


Figure 1. Void abundance in the sub-sampled cold dark matter field of the `DEMNUni` simulation. Colors denote the sum of neutrino masses used in each simulation. The bottom panel shows the ratio between void number densities (with uncertainties) for different Σm_ν values and the number density in the massless neutrino case. Increasing Σm_ν increases the number of small voids and decreases the number of large voids derived from the particle field. All abundance plots are cut at ~ 2 times the mean particle separation in the simulation and where voids are so large that there are too few voids for informative uncertainties. All figures are for $z = 0$.

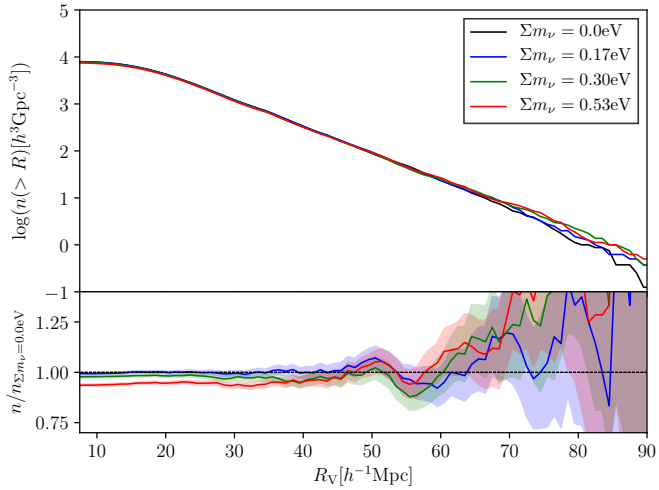


Figure 2. Void abundance in the halo field of the `DEMNUni` simulation. Colors denote the sum of neutrino masses used in each simulation. The bottom panel shows the ratio between void number density with uncertainties for the different Σm_ν values and the number density in the massless neutrino case. Increasing Σm_ν decreases the number of small voids and increases the number of large voids derived from the halo field.

runs on a tracer distribution and uses the position of these objects, we can find voids from both the halo distribution (in this work we use the friends-of-friends (FoF) catalogs) and the CDM particle distribution. For the latter, running the void finding procedure on a large number of CDM particles (e.g. directly on the 2048^3 particles) is computationally expensive. We thus subsampled the CDM particle field to 1.5% of the original particle number for both `DEMNUni` and `MassiveNuS`. See Sutter et al. (2014a) for a discussion on how subsampling the tracer distribution affects voids. We note that for the `DEMNUni` subsampling this corresponds roughly to 505^3 particles, which is comparable to the CDM particle number density in the work done by Massara et al. (2015). Throughout the paper we refer to the subsampled CDM particle field simply as "CDM particles". We do not subsample the halo field unless specified. See Appendix A for more information on the simulations and void finder.

3 RESULTS

The sum of neutrino masses affects both the number of voids and the void bias. As the sum of neutrino masses increases, there are fewer large voids and more small voids seen in the CDM field. However, if we use halos as tracers there are more large voids and fewer small voids. The total number of voids changes, as well (see Section 3.1). Neutrinos affect how voids cluster and produce a strong scale dependent trend– this is a distinctive feature (see Section 3.2).

We note that we have also analyzed void catalogs built from the mock HOD[3] galaxy catalog obtained from the DEMNUni simulations. The HOD's are built using the model described in Zheng et al. (2005), and the luminosity dependence is described in de la Torre et al. (2013). Results for the HOD catalogs are consistent with those obtained for the halo field. From now on we focus our analysis only on void catalogs extracted from the CDM and halo fields.

3.1 Void abundance

The impact of Σm_ν on the void abundance, i.e. the void size function, depends upon the tracer. In Figure 1 and Figure 2 we show the void abundances derived from the subsampled CDM distribution and the halo distribution, respectively, for the `DEMNUni` simulation. All abundance plots have Poisson uncertainties.

The trend with Σm_ν for the void abundance derived from the halo distribution is inverted relative to that derived from the CDM particle field. The void abundance derived from the CDM field shows that increasing Σm_ν increases the number of small voids and decreases the number of large voids. Our findings are consistent with Massara et al. (2015)'s results based on a simulation with lower volume and mass resolution than `DEMNUni`. Conversely, for the void abundance derived from the halo distribution (see Figure 2) increasing Σm_ν *decreases* the number of small voids and *increases* the number of large voids, although the magnitude of the effect is lower in absolute value than in the CDM case. As explained in Appendix B, although the number density

[3] Contact Adam Hawken for the HOD code at adamhawken@gmail.com

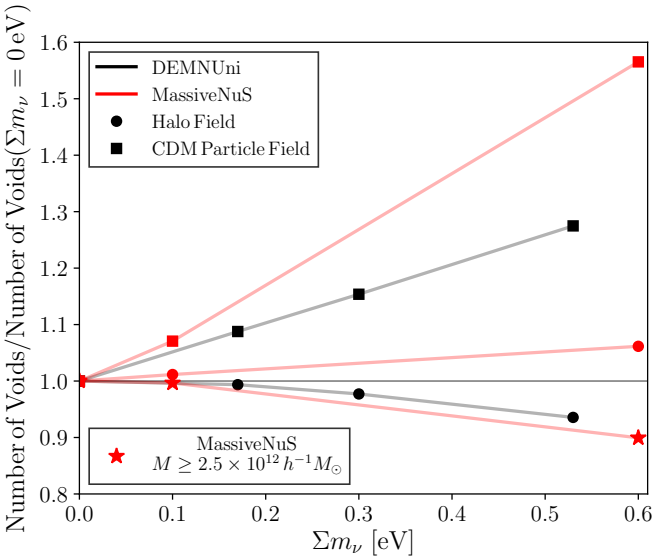


Figure 3. The total number of voids for each simulation and each tracer as a function of the sum of neutrino masses. The number is normalized to the number of voids in the simulation when $\Sigma m_\nu = 0$ eV. The normalization values are 63822, 441174, 4765, and 22337 for the `DEMNUni` halos case, `DEMNUni` CDM case, `MassiveNuS` halos case, and `MassiveNuS` CDM case, respectively. The total number of voids increases with Σm_ν for voids traced by cold dark matter and decreases with Σm_ν for voids traced by halos with a high mass threshold. The range of Σm_ν spans values covered by the simulations in our analysis.

of the tracers changes when changing Σm_ν, the number density is not the origin of the opposite trends observed in the different void abundance plots.

Previous simulations lacked a sufficient combination of volume and mass resolution to investigate the void abundance derived from the halo field in detail and so were unable to discriminate between these two different trends in the void statistics (see e.g. Section 5 of Massara et al. 2015, whose simulations had 512^3 CDM particles, 512^3 neutrinos, and a $500\,h^{-1}$Mpc box length).

Varying Σm_ν not only impacts the void abundance but also the total number of voids, as expected. In Figure 3 we show the total number of voids in the `DEMNUni` and `MassiveNuS` simulations derived from both the halo distribution and CDM particle distribution as a function of Σm_ν. For voids derived from the CDM distribution, the total number of voids increases as Σm_ν increases. There are more small voids and less large voids for the CDM case as Σm_ν increases. The simulation volume is kept fixed, so overall there is a larger total number of voids that fill the volume.

For the halo case, the `DEMNUni` and `MassiveNuS` simulations show opposite behavior for the total number of voids as a function of Σm_ν. Increasing Σm_ν decreases the total number of `DEMNUni` voids derived from the halo field. This occurs because increasing Σm_ν decreases the number of small voids and increases the number of large voids in the `DEMNUni` halo case, so there must be a lower (with respect to the massless neutrino case) total number of voids to fill the simulation volume. For the `MassiveNuS` simulations, the number of voids increases with Σm_ν in both the halo and CDM cases. The `MassiveNuS` simulations have a smaller volume than the `DEMNUni` simulation, yielding a smaller total number of voids and, thus, larger uncertainties in the void abundance than the `DEMNUni` simulation. Nonetheless, the `MassiveNuS` void abundances for both the halo case and CDM case appear to be consistent with the trends seen in the `DEMNUni` CDM case. Thus, since the `MassiveNuS` simulation has more small voids for both the halo case and CDM case for nonzero Σm_ν relative to the massless case, the total number of voids must also increase with Σm_ν in both cases. We include the `MassiveNuS` void abundances in Appendix C. `MassiveNuS` has halos with smaller masses than `DEMNUni`, and thresholding the halo mass in `MassiveNuS` to match that of `DEMNUni` gives concordance between the two simulations for the total number of voids traced by halos. We also test different halo mass cuts in the halo catalogs and discuss the number of voids for the mass cut `MassiveNuS` simulation in Section 3.2 and comment further on these trends in Section 4.

3.2 Power Spectra & Correlation Functions

The void distribution is sensitive to Σm_ν and how Σm_ν impacts the underlying tracer distribution. Increasing the sum of neutrino masses damps the CDM power spectrum, $P_{\rm cc}$, on small scales in the `DEMNUni` simulation, as expected since neutrinos do not cluster on scales smaller than their free-streaming length (Lesgourgues & Pastor 2006). As Σm_ν increases, the effect becomes more significant.

The halo-halo power spectrum, $P_{\rm hh}$, for `DEMNUni` shows an overall boost in power as Σm_ν increases and biases the halo distribution (see Figure 4, all power spectra have a k bin size $\Delta k \approx 0.008\,h$Mpc^{-1} unless otherwise noted and have uncertainties computed by `VIDE` and estimated from scatter in the bin average). Neutrinos reduce the growth of CDM perturbations. Therefore, at a fixed redshift, virialized halos have a smaller mass than in the massless neutrino case at the same redshift. The densest initial fluctuations in the matter density field will still form halos large enough to be detected in our simulations, but, depending on the value of Σm_ν, fluctuations with sufficiently low densities will no longer form halos with masses above the simulation mass threshold. Because only halos at the densest overdensities can be detected in simulations, halos at all scales are more highly correlated (with respect to the massless neutrino case), leading to a larger halo bias $b_{\rm h}$. The larger halo bias tends to compensate the suppression of the matter power spectrum due to free-streaming neutrinos, and the cumulative effect depends on Σm_ν. The halo power spectrum is given by:

$$P_{\rm hh} = b_{\rm h}^2 P_{\rm cc}, \tag{1}$$

where, in the presence of massive neutrinos, $b_{\rm h}$ is defined with respect to the cold dark matter density (Castorina et al. 2014). The impact of the sum of neutrino masses on halo bias has been a topic of intense and ongoing study (see e.g. De Bernardis et al. 2008; Marulli et al. 2011; Villaescusa-Navarro et al. 2014; Castorina et al. 2014, 2015; Biagetti et al. 2014; Loverde 2014; Massara et al. 2014; Petracca et al. 2016; Loverde 2016; Desjacques et al. 2016; Raccanelli et al. 2017; Vagnozzi et al. 2018). We note that a similar inversion in the effect of the sum of neutrino masses on the matter power spectrum and the halo power spectrum has been seen

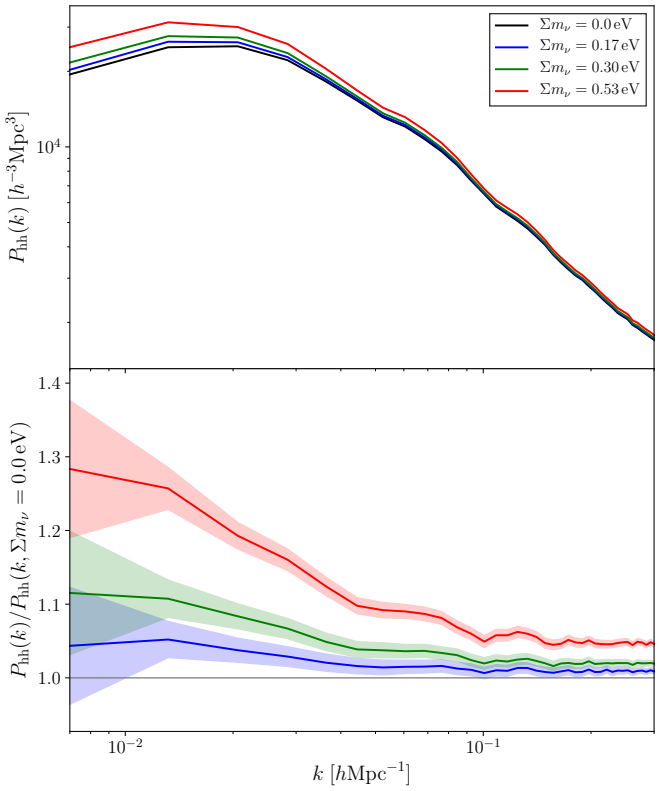


Figure 4. The halo-halo power spectrum for the `DEMNUni` simulation. Colors denote the sum of neutrino masses used in each simulation. The bottom panel shows the ratio between the different Σm_ν cases and the massless case. Increasing Σm_ν induces a biasing effect that *boosts* the power spectrum. The power spectrum spans the scales accessible to the `DEMNUni` simulation.

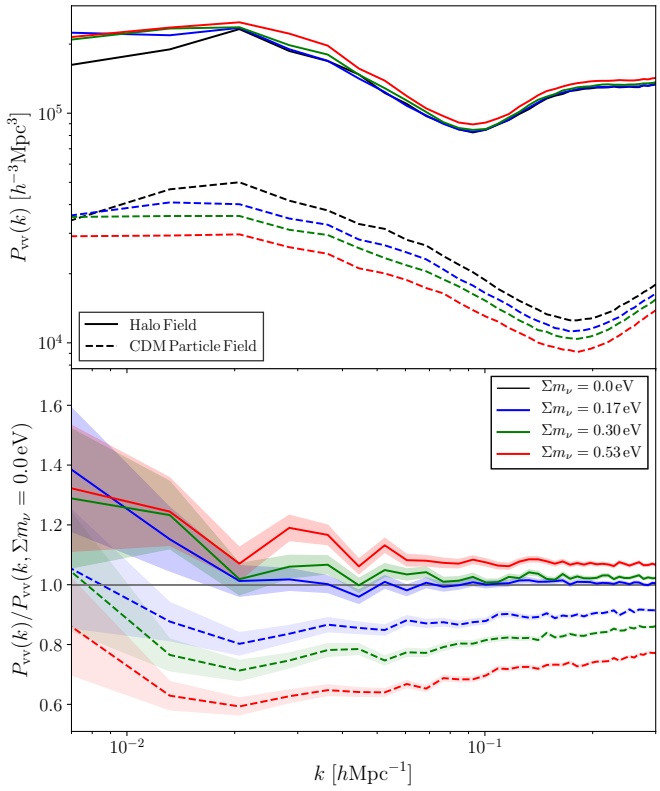


Figure 5. Void-void power spectrum for the `DEMNUni` simulation. Colors denote the sum of neutrino masses used in each simulation, dashed denotes voids traced by the CDM particle field, and solid denotes voids traced by the halo field. The bottom panel shows the ratio between the different Σm_ν cases and the respective massless case. Increasing Σm_ν *boosts* the power spectrum for voids derived from the halos but *damps* the power spectrum for voids derived from the particle distribution. The power spectrum spans the scales accessible to the `DEMNUni` simulation.

by Marulli et al. (2011) (see also Villaescusa-Navarro et al. 2014; Castorina et al. 2014).

We find that increasing Σm_ν boosts the correlation between voids derived from the halo distribution while it damps the correlation between voids derived from the CDM particle field for the DEMNUni simulation (see Figure 5).

To understand the effects of halo mass on the power spectra in the presence of neutrinos, we analyze the void distribution in the `MassiveNuS` simulations, which have a lower halo mass threshold. We plot the halo-halo power spectra and the void-void power spectra, as a function of Σm_ν in Figure 6 and Figure 7, respectively. The `MassiveNuS` simulations do not show the overall boost in the halo power for increasing Σm_ν that we see in the `DEMNUni` halo distribution. The void-void power spectra show a similar trend: for the `MassiveNuS` simulations, the power spectra of voids found in the halo distribution behave as the power spectra of voids derived from the CDM particle field, even if the differences due to neutrinos effects are much less pronounced in the former than in the latter. In other words, the `MassiveNuS` void spectra *do not show the same inversion* between the halo and CDM cases as that observed in the `DEMNUni` simulations. We discuss the physical explanation behind this *apparent* contradiction in Section 4.

3.2.1 The Effects of Tracer Bias

While on the one hand neutrinos have a physical impact on the total number of voids (see Section 3.1), on the other hand the number of voids directly maps to the void shot noise, which can be approximated at small scales as $1/n_{\rm v}$, where $n_{\rm v}$ = (Number of Voids)/Volume is the void density.

To disentangle the impacts on the void power spectra of the void number and halo bias as they change with Σm_ν, we remove shot noise and subsample the `DEMNUni` simulation in two different manners:

(i) we bias the halo distribution by making two mass cuts such that each of them contains only halos with $M \geq 5 \times 10^{12}\,h^{-1}M_\odot$ or $M \geq 1 \times 10^{14}\,h^{-1}M_\odot$;

(ii) we randomly subsample the halo distribution so that the number of halos matches that of the two subsamples defined in (i). In this way we produce sub-sets of halos with the same bias as the full halo distribution of the `DEMNUni` simulations, but with the same halo number density as the highly biased subsamples in (i) (see e.g. Figure B2 in Appendix B for a similar application to the `MassiveNuS` simulations).

To remove the effects of void number density we model

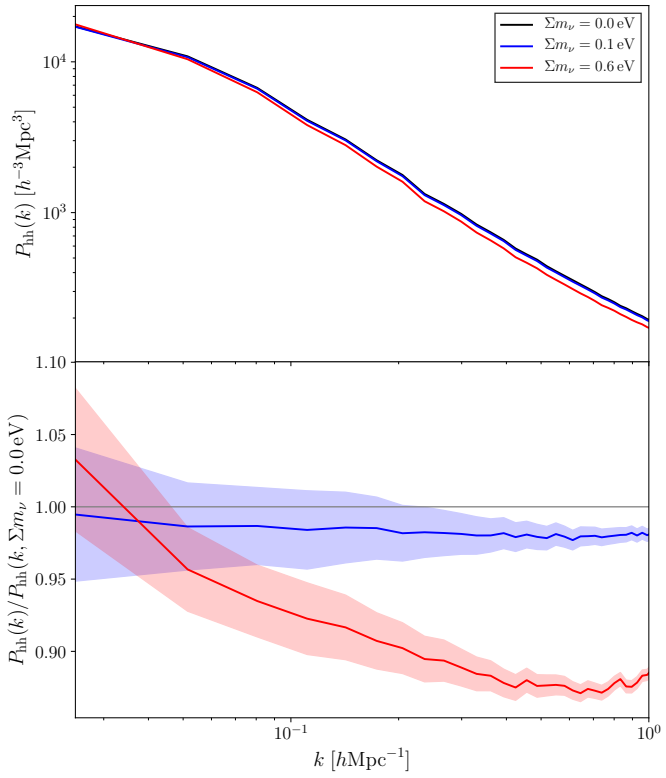


Figure 6. The halo-halo power spectrum for the `MassiveNuS` simulation. Colors denote the sum of neutrino masses used in each simulation. The bottom panel shows the ratio between the different Σm_ν cases and the massless case. Increasing Σm_ν *damps* the power spectrum, in contrast to the effect on the `DEMNUni` power spectrum. This is because `MassiveNuS` has a lower mass threshold ($M_{\rm min} = 3 \times 10^{11}\, h^{-1} M_\odot$) than `DEMNUni` ($M_{\rm min} = 2.5 \times 10^{12}\, h^{-1} M_\odot$). The power spectrum spans the scales accessible to the `MassiveNuS` simulation, which are smaller than those for the `DEMNUni` simulation since `MassiveNuS` has a smaller volume and larger resolution.

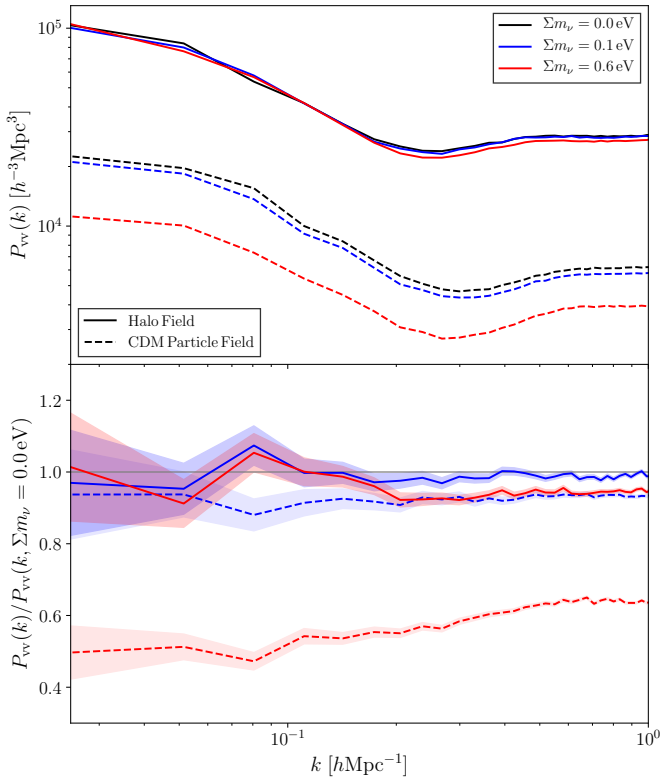


Figure 7. The void-void power spectrum for the `MassiveNuS` simulation for voids derived from the halo distribution. Colors denote the sum of neutrino masses used in each simulation. The bottom panel shows the ratio between the different Σm_ν cases and the massless case. Increasing Σm_ν *damps* the power spectrum, in contrast to the effect on the `DEMNUni` power spectrum. We interpret this as due to the bias of the tracer population used to define voids (see Section 3.2). The power spectrum spans the scales accessible to the `MassiveNuS` simulation.

the shot noise for the void-void power spectrum as scale-dependent following the prescription by Hamaus et al. (2014a), which is well approximated by $1/n_{\rm v}$ for small scales:

$$\mathcal{E}_{\rm vv}(k) = P_{\rm vv} - \frac{P_{\rm vc}^2}{P_{\rm cc}}, \tag{2}$$

where $P_{\rm vv}$ is the void-void power spectrum and $P_{\rm vc}$ is the void-CDM cross-correlation power spectrum. Thus, we can write the void power spectrum with shot noise removed as

$$P_{\rm vv,\,no\,shot}(k) = \frac{P_{\rm vc}^2}{P_{\rm cc}}. \tag{3}$$

The sum of neutrino masses affects the amplitude and phase of the void-void power spectrum. In Figure 8 we plot the void power spectra (with shot noise removed) for the two highly biased catalogs of (i), and compare them with the void spectra of the corresponding randomly subsampled catalogs of (ii) (see Figure B3 in Appendix B for analogous void power spectra including shot noise for multiple halo mass thresholds from `MassiveNuS`). At large scales, the void power spectrum tracks the tracer power spectrum: the power at large scales for the voids traced by halos with a higher mass threshold is larger, as expected for a more biased sample. Nonetheless, the large scale power is of the same order of magnitude for both the mass thresholds at large scales (compare top and bottom panels of Figure 8). For the highly biased tracers ($M \geq 1 \times 10^{14}\, h^{-1} M_\odot$, bottom panel), the power at large scales is dominated by uncertainties because there are less small voids that correlate at large scales. For the less highly biased tracers ($M \geq 5 \times 10^{12}\, h^{-1} M_\odot$, top panel) there is a discernible difference for the two neutrino masses at large scales because there is a large number of small voids traced by smaller halos, improving the uncertainties.

The power at small scales dramatically increases with Σm_ν when increasing the halo bias (compare top and bottom panels of Figure 8). The small voids that remain when increasing Σm_ν have highly biased halos forming their walls. These highly biased halos sit near overdensities, forming a concentrated cosmic web with voids that are, thus, tightly packed, boosting their correlation. The minimum at scales just larger than $k = 10^{-1}\, h\mathrm{Mpc}^{-1}$ corresponds to the scale at which voids are uncorrelated (see e.g. Hamaus et al. 2014a). The scale of the local maximum to the right of this minimum corresponds to the void exclusion scale, $k_{\rm exc} \approx \pi/\bar{R}_{\rm v}$, where $\bar{R}_{\rm v}$ is the average void radius. This is the smallest scale at

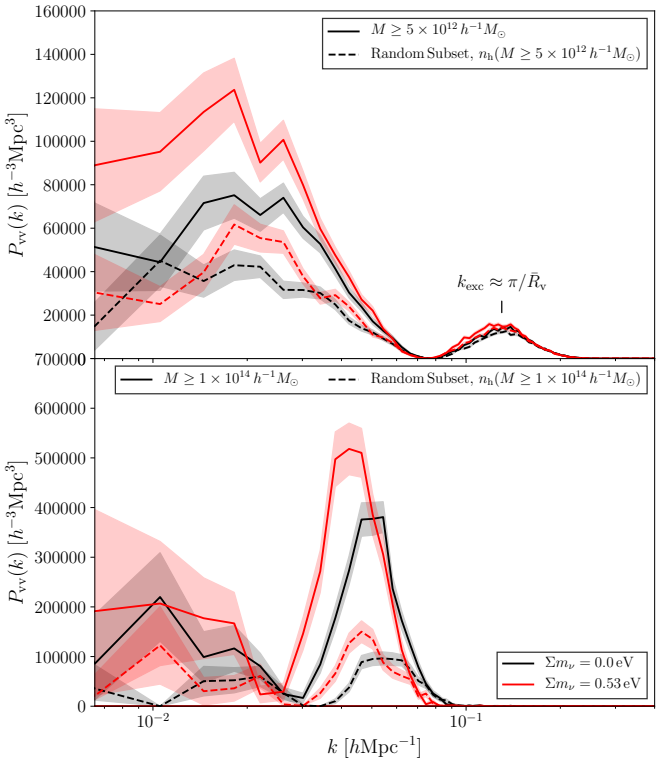


Figure 8. The void-void power spectrum with shot noise removed for the `DEMNUni` simulation for voids derived from the halo distribution. Removing shot noise removes the effects of void number density. Colors denote the sum of neutrino masses used in each simulation. The top panel corresponds to voids found in the less highly biased tracer field, while the bottom panel corresponds to voids found in the highly biased tracer field. Dashed lines correspond to randomly subsampling the original halo catalog so its number density matches that of the mass thresholded catalog, removing the effects of tracer density. The impact of Σm_ν on void clustering depends on halo bias.

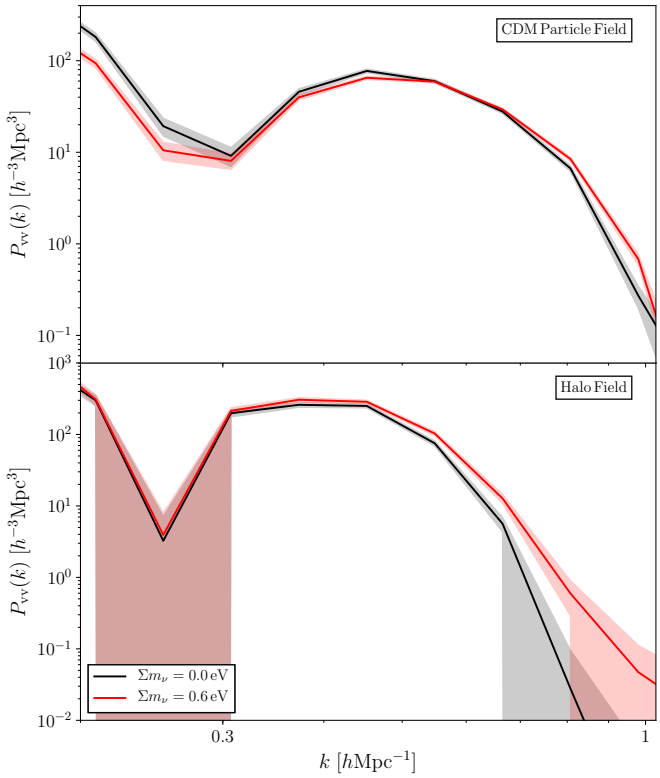


Figure 9. The void-void power spectrum near the exclusion scale with shot noise removed for the `MassiveNuS` simulation. Colors denote the sum of neutrino masses used in each simulation. The top panel corresponds to voids found in the CDM particle field, while the bottom panel corresponds to voids found in the halo field. The low mass threshold $M \geq 3 \times 10^{11}\,h^{-1}M_\odot$ for `MassiveNuS` causes voids traced by the halos to behave similar to voids traced by the CDM particles for small scales.

which voids with radius $\bar{R}_v$ do not overlap (Hamaus et al. 2014a).

Increasing Σm_ν shifts the power from small scales to large scales for the `DEMNUni` voids found in the halo distribution. Σm_ν may create a scale-dependent bias in voids, but this effect must be more thoroughly investigated to determine if the scale dependence is due to neutrino properties, non-linearities, or other effects. Increasing the halo bias increases the scale-dependent impact Σm_ν has on the void power spectra. This is seen most clearly near the void exclusion scale. This shift in power from small voids to large voids is consistent with Σm_ν decreasing the number of small voids and increasing the number of large voids for voids derived from the halo distribution in the `DEMNUni` simulations, thus causing the average void radius to increase and $k_{\rm exc}$ to decrease (see Section 3.1).

On the other hand we find that, for the `MassiveNuS` simulations, increasing Σm_ν shifts the power in the void power spectra (with shot noise removed) from large to small scales for both the CDM voids and halo voids (see near the exclusion scale $k \approx 0.5\,h\mathrm{Mpc}^{-1}$ in Figure 9, which has bin size $\Delta \log k \approx 0.08\,h\mathrm{Mpc}^{-1}$). This is in contrast to the shift in power from small to large scales seen for the `DEMNUni` simulation in Figure 8. We note that the `DEMNUni` void power spectra (with shot noise removed) for CDM voids is consistent with that of `MassiveNuS`.

Tracer bias influences how different kinds of voids respond to Σm_ν: a low mass threshold, and so a low tracer bias, does not produce an inversion between the CDM case and halo case for the void abundance and power spectra. We have verified that sampling the `MassiveNuS` halo distribution so it has the same minimum halo mass as the `DEMNUni` simulation, $M \geq 2.5 \times 10^{12}\,h^{-1}M_\odot$ and thus increasing the tracer bias, leads to the inverted behavior between the biased halo case and the CDM case for the abundances, total number of voids (see Figure 3), and the power spectra, like seen for the `DEMNUni` simulation. The exclusion scale in the biased `MassiveNuS` distribution also shifts from small scales to match the `DEMNUni` exclusion scale.

The correlation functions are a useful tool to view the Σm_ν inversion effects in real space. In Figure 10 we plot the void auto-correlation function for voids derived from the CDM particle field and the halo field. All correlation functions are computed by `VIDE` via an inverse Fourier transform

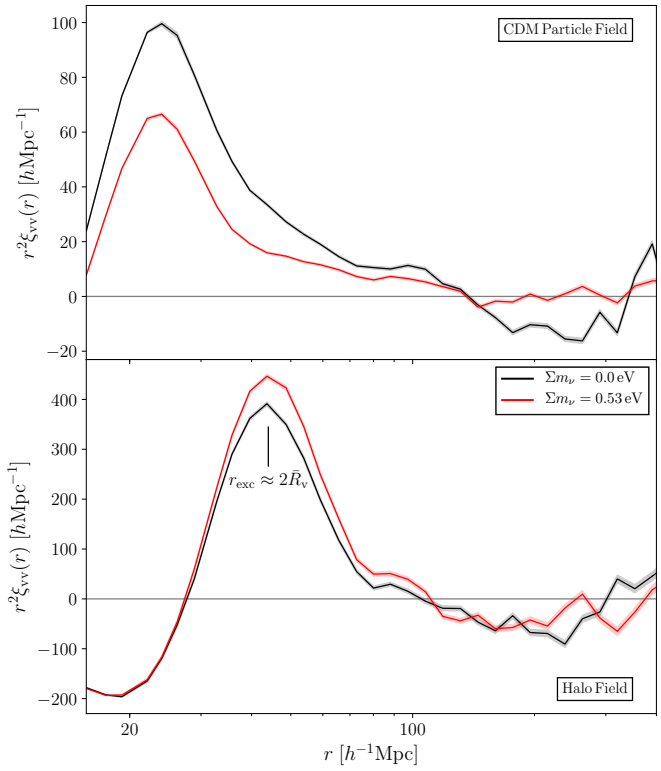


Figure 10. The void auto-correlation function for `DEMNUni` voids, including uncertainties. We scale the correlation functions by r^2 to emphasize the effects at large r. Colors denote the sum of neutrino masses used in each simulation. The top panel corresponds to voids found in the CDM particle field, while the bottom panel corresponds to voids found in the halo field. Increasing Σm_ν diminishes void clustering for voids traced by CDM particles while it enhances void clustering for voids traced by halos. All correlation functions are cut at 2 times the mean particle separation in the simulation and where scales are so large that noise dominates. Voids traced by the CDM particles are so small that the correlation function does not become negative for scales larger than 2 times the particle separation due to the simulation resolution.

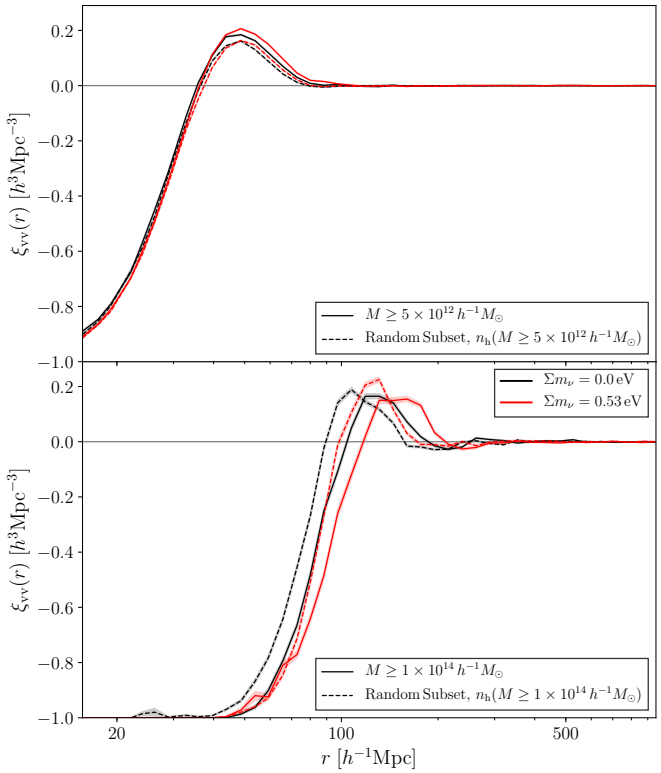


Figure 11. The void auto-correlation function for the `DEMNUni` simulation for voids derived from the halo distribution, including uncertainties. Colors denote the sum of neutrino masses used in each simulation. The top panel corresponds to voids found in the less highly biased tracer field, while the bottom panel corresponds to voids found in the highly biased tracer field. Increasing Σm_ν shifts the correlation peak to larger scales and boosts the correlation. Increasing the halo bias amplifies the effect of Σm_ν on void clustering.

of the power spectra, have an r bin size $\Delta \log r \approx 0.04\,h^{-1}$Mpc, and have uncertainties computed by `VIDE` and estimated from scatter in the bin average. ξ_{vv} peaks at the void exclusion scale $2\bar{R}_{\mathrm{v}}$ because this is the average distance at which voids are most tightly packed, i.e. the walls of neighboring spherical voids with a radius equal to the average void radius meet. ξ_{vv} decreases for smaller scales, i.e. scales smaller than $2\bar{R}_{\mathrm{v}}$, since voids do not overlap. As explained in Massara et al. (2015), this decline is gradual because voids are not perfect spheres and they have different sizes. For scales larger than the exclusion scale, voids do not cluster as much and so ξ_{vv} falls. We note that the void auto-correlation function becomes negative at scales larger than the Baryon Acoustic Oscillations (BAO) before approaching zero since voids trace the matter distribution at large scales. Voids are not likely to be separated by this distance.

Increasing Σm_ν suppresses void clustering for the CDM case at scales smaller than the BAO peak position, and reduces the anticorrelation at large scales since there are more voids spread throughout the field. Voids derived from the halos cluster more near the exclusion scale, showing opposite behavior to the CDM case just like the power spectra.

In the upper panel of Figure 11 we compare, for two different values of Σm_ν, voids derived from the less highly biased halo catalog defined in (i) to the corresponding catalog, defined in (ii), derived from the original halo catalog with the same halo density for two different Σm_ν. Increasing Σm_ν boosts the correlation of voids derived from the biased halo sample, analogous to the effect on halos with large bias. Increasing the neutrino mass reduces the number of small voids traced by halos in the field, so the remaining voids are more highly correlated, resulting in a higher correlation peak. Since there are less small voids and more large voids, there is more void clustering for scales larger than the exclusion scale.

Σm_ν's impacts on the amplitude and scale are most prominent for voids traced by highly biased tracers. In the lower panel of Figure 11 we show the void auto-correlation function for voids derived from the highly biased halo sample and the original catalog with the same halo density. Decreasing the tracer density and increasing the halo bias both shift the average void radius to larger scales, causing the corre-

lation function to peak at larger scales (compare upper and lower panels). For the voids traced by the less dense and highly biased halos, increasing Σm_ν strongly shifts the entire correlation function to larger scales, similarly to the impact on the power spectra in Figure 8.

The impact of Σm_ν on the correlation functions is not simply explained by the effects of void abundance. In the upper panel of Figure 11 we see that increasing Σm_ν boosts the correlation for the voids traced by the less highly biased halos without significantly changing the peak location relative to the massless case. On the contrary, for the highly biased case in the lower panel of Figure 11, the amplitude at the correlation peak does not change between the massless and $\Sigma m_\nu = 0.53\,\mathrm{eV}$ cases. If void abundance solely drove Σm_ν's impacts on the correlation functions, the correlation peak's amplitude would decrease as the average void radius increases (see e.g. the void auto-correlation functions in Massara et al. 2015, for different void sizes). Neutrinos impact the clustering of voids – Σm_ν influences void bias. We further explore the impact of Σm_ν in our upcoming paper.

4 DISCUSSION

Our work indicates that voids respond to Σm_ν in two distinct manners, determined by if they are derived from the halo distribution or the cold dark matter particle field. Both the halo and CDM distributions should be utilized to properly study voids and the impact neutrinos have on them. For forecasting constraints on Σm_ν, the void catalog ideally should be built from the survey mock or HOD populated simulation rather than the CDM distribution.

Increasing Σm_ν slows down the growth of the CDM perturbations, reducing the CDM overdensities present today. Since the evolution of the overdensities has slowed, fewer mergers of the small overdensities have occurred, resulting in a larger number of small CDM overdensities and fewer large CDM overdensities relative to the massless neutrino case. The numerous smaller CDM overdensities yield smaller voids since the small overdensities fragment what would be large voids. Hence, increasing Σm_ν increases the number of small voids and decreases the number of large voids derived from the CDM particle field. Since there are more small overdensities in the field as Σm_ν increases, voids become less biased near the correlation peak since they are not as localized and less antibiased for scales larger than the BAO peak position, as it is more likely to find voids separated by larger distances.

We note that our void finding procedure in the CDM case only uses CDM particles and does not include the neutrino particles. A different approach is to locate voids in the total matter field, such as in the work of Banerjee & Dalal (2016) that included neutrino particles and CDM particles. In our work, we have established that the inversion is unique to voids derived from halos because halo bias drives the inversion. Therefore, our results are particularly relevant to interpreting void observations.

For the halo case, increasing Σm_ν makes halos less massive, leaving only the halos that sit at large density perturbations detectable in our simulations. Thus, these halos are more highly correlated and we see a bias effect in the halo-halo power spectra. For the `DEMNUni` simulation, only massive halos remain due to the limited mass resolution of the simulations, so there are no longer small halos that could segment a larger void into separate voids. For this reason and since larger voids are defined by larger overdensities, increasing Σm_ν increases the number of large voids derived from the halo catalog and decreases the number of small voids.

The high resolution of the `MassiveNuS` simulation produces a lower minimum halo mass and, thus, halos that are less biased tracers of the CDM particle field than the `DEMNUni` simulation. `MassiveNuS` can identify halos at smaller CDM overdensities than `DEMNUni`, and, consequently, these halos have masses and bias lower than the `DEMNUni` mass resolution. However, `MassiveNuS` has a finite resolution and cannot identify halos at the smallest CDM overdensities, so its halo catalog is still biased (even if its effective bias is smaller than the `DEMNUni` halo catalogs), and its halos have a higher correlation than the CDM overdensities.

Since increasing Σm_ν leads to more small CDM overdensities and `MassiveNuS` has a low effective halo bias, `MassiveNuS` halos trace these small CDM overdensities more than the `DEMNUni` halos. Halos in `MassiveNuS` are less biased tracers of the matter density field; therefore, the increased correlation due to the halo's bias from the simulation resolution and Σm_ν is not substantial enough to overpower the damping effects from the neutrino free-streaming. Thus, the `MassiveNuS` void power spectra for voids found in the CDM field and for voids found in the halo field damp as Σm_ν increases.

5 CONCLUSIONS & FUTURE PROSPECTS

We have explored the impact of the sum of neutrino masses Σm_ν on void properties with the N-body simulations `DEMNUni` and `MassiveNuS`. For the first time we have shown that:

(i) the effect Σm_ν has on void properties depends on the type of tracer the void catalog was built from,

(ii) using voids only derived from the cold dark matter particle field to study neutrinos, as has been assumed in the literature, is not sufficient to capture the effects of neutrinos on voids. Voids are not always smaller and denser in the presence of neutrinos, and tracer properties can actually lead to larger voids, a smaller number of voids, and enhanced void clustering,

(iii) the impact of Σm_ν on the void abundance and void-void power spectrum for the `DEMNUni` void catalog derived from the halo distribution is opposite to that for the void catalog derived from the CDM particle field. For voids derived from the cold dark matter field, increasing Σm_ν increases the number of small voids, decreases the number of large voids, and damps the void-void power spectrum. The opposite is true for voids derived from the biased halo distribution due to the effects of halo bias,

(iv) halo bias influences how Σm_ν affects voids – this will have interesting impacts on future surveys aiming to constrain the sum of neutrino masses, and

(v) void power spectra and auto-correlation functions are powerful tools for distinguishing neutrino masses. Neutrinos leave a distinct fingerprint on voids, which can potentially help break the degeneracy between cosmological parameters

in halo measurements. We plan to thoroughly explore breaking degeneracies, such as σ_8, in upcoming work.

By comparing observations of the number of voids, void abundance, and void clustering to ΛCDM simulations with volume and resolution matching the survey volume and galaxy number density, surveys have a new avenue to place constraints on Σm_ν. Upcoming surveys like PFS, DESI, Euclid, and WFIRST have halo densities near that of `DEMNUni`, and the densest may even exceed the density of `DEMNUni`. For these upcoming observations, simulations such as `DEMNUni` and `MassiveNuS` are the best tools for evaluating the impact of neutrinos on the observed voids. In the final stages reliable mocks will also be necessary to correctly evaluate the mask and survey boundary effects.

The opposite behavior of the `DEMNUni` and `MassiveNuS` simulation to Σm_ν indicates there exists a threshold halo bias for which the void power spectra, correlation functions, and abundances for voids derived from the halo distribution will be less sensitive to Σm_ν. It would be interesting to compare surveys with halo biases above and below the threshold at which Σm_ν induces the inversion effect in the void abundances, number, power spectra, and correlation functions, since lower densities increase the minimum halo mass, and so halo bias, of the survey. In this sense one could imagine an extraordinarily dense low-z survey to be particularly interesting. Within the same survey, it will be interesting to compare void properties for tracers with different luminosity or mass thresholds, i.e. with different biases. The use of multi-tracer techniques is another promising tool for constraining Σm_ν and its impact on voids. Utilizing the redshift dependence of these effects and redshift coverage of these surveys could further yield unique constraints on neutrino properties. We explore this interdependence in our upcoming paper.

ACKNOWLEDGEMENTS

We thank F. Villaescusa-Navarro and J. Bel for useful discussions and comments on the manuscript. CDK is supported by the National Science Foundation Graduate Research Fellowship under Grant DGE 1656466. AP and EM are supported by NASA grant 15-WFIRST15-0008 to the WFIRST Science Investigation Team "Cosmology with the High Latitude Survey". The DEMNUni-I simulations were carried out at the Tier-0 IBM BG/Q machine, Fermi, of the Centro Interuniversitario del Nord-Est per il Calcolo Elettronico (CINECA, Bologna, Italy), via the ve million cpu-hrs budget provided by the Italian SuperComputing Resource Allocation (ISCRA) to the class-A proposal entitled "The Dark Energy and Massive-Neutrino Universe". C.C. acknowledges financial support from the European Research Council through the Darklight Advanced Research Grant (n. 291521). JL is supported by an NSF Astronomy and Astrophysics Postdoctoral Fellowship under award AST-1602663. This work used the Extreme Science and Engineering Discovery Environment (XSEDE), which is supported by NSF grant ACI-1053575. The `MassiveNuS` simulations are publicly available at `http://columbialensing.org` through the Skies & Universes Project. This work has been done within the Labex ILP (reference ANR-10-LABX-63) part of the Idex SUPER, and received financial state aid managed by the Agence Nationale de la Recherche, as part of the programme Investissements d'avenir under the reference ANR-11-IDEX0004-02. The Flatiron Institute is supported by the Simons Foundation.

APPENDIX A: SIMULATION AND VOID FINDER DETAILS

A1 The `DEMNUni` simulation suite

The `DEMNUni` simulations have been performed using the tree particle mesh-smoothed particle hydrodynamics (TreePM-SPH) code GADGET-3 Springel et al. (2001), specifically modified by Viel et al. (2010) to account for the presence of massive neutrinos. They are characterized by a softening length $\varepsilon = 20$kpc, start at $z_{\rm in} = 99$, and are performed in a cubic box of side $L = 2000\,h^{-1}$Mpc, containing $N_{\rm p} = 2048^3$ CDM particles, and an equal number of neutrino particles when $\Sigma m_\nu \neq 0$ eV. These features make the `DEMNUni` set suitable for the analysis of different cosmological probes, from galaxy-clustering, to weak-lensing, to CMB secondary anisotropies.

Halos and sub-halo catalogs have been produced for each of the 62 simulation particle snapshots, via the friends-of-friends (FoF) and SUBFIND algorithms included in Gadget III Springel et al. (2001); Dolag et al. (2010). The linking length was set to be 1/5 of the mean inter-particle distance (Davis et al. 1985) and the minimum number of particles to identify a parent halo was set to 32, thus fixing the minimum halo mass to $M_{\rm FoF} \simeq 2.5 \times 10^{12}\ h^{-1} M_\odot$.

A2 The `MassiveNuS` simulation suite

The `MassiveNuS` simulations consists a large suite of 101 N-body simulations, with three varying parameters Σm_ν, A_s, and Ω_m. In order to avoid shot noise and high computational costs typically associated with particle neutrino simulations, `MassiveNuS` adopts a linear response algorithm (Ali-Haïmoud & Bird 2013), where neutrinos are described using linear perturbation theory and their clustering is sourced by the full non-linear matter density. This method has been tested robustly against CDM particle simulations and agreements are found to be within 0.2% for $\Sigma m_\nu \leq 0.6$ eV.

The simulations use the public code `Gadget-2`, patched with the public code `kspace-neutrinos` to include neutrinos[4]. The `MassiveNuS` halo catalogues are computed using the public halo finder code `Rockstar`[5] (Behroozi et al. 2013), also a friends-of-friends-based algorithm.

A3 Void finder

`VIDE` performs a Voronoi tessellation of the tracer field, creating basins around local minima in the density field. It then relies on the Watershed transform (Platen et al) to merge basins and construct a hierarchy of voids. `VIDE` has been

[4] The code also has the flexibility to include neutrinos as particles at low redshifts, to capture neutrino self-clustering. The latest version may be found here: `https://github.com/sbird/kspace-neutrinos`

[5] `https://bitbucket.org/gfcstanford/rockstar`

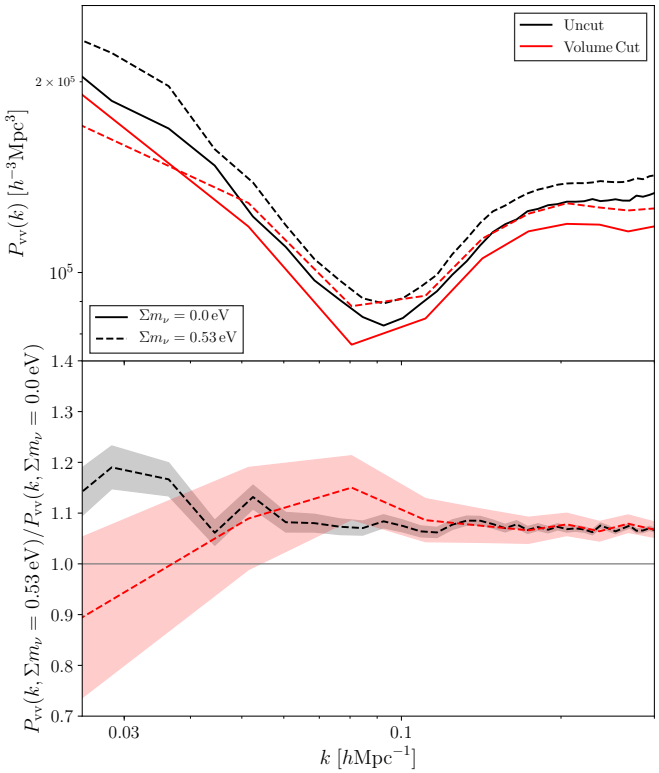


Figure B1. Void-void power spectra for voids derived from the DEMNUni halo distribution. Black spectra correspond to the original uncut DEMNUni simulation, while red spectra correspond to the volume cut DEMNUni simulation. Solid lines correspond to $\Sigma m_\nu = 0.0\,\mathrm{eV}$ while dashed lines correspond to $\Sigma m_\nu = 0.53\,\mathrm{eV}$. The bottom panel shows the ratio, with respect to the massless neutrino case, for the uncut and volume cut simulations. The volume cut and uncut simulations are equivalent within uncertainties, so the volume differences between DEMNUni and MassiveNuS do not induce the inversion.

widely used in recent cosmological analysis (e.g. Sutter et al. (2012); Pisani et al. (2014); Sutter et al. (2014d); Hamaus et al. (2014c, 2016, 2017); Pollina et al. (2017)) and embeds the ZOBOV code (Neyrinck 2008).

With VIDE we define the void radius as:

$$R_\mathrm{V} \equiv \left(\frac{3}{4\pi}V\right)^{1/3} \tag{A1}$$

where the volume V is the total volume of all the Voronoi cells composing the void (following VIDE's convention). It is important to notice that VIDE is able to find voids regardless of the shape, so it is particularly adapted to correctly capture the non-spherical feature of voids.

APPENDIX B: ROBUSTNESS TO VOLUME AND RESOLUTION EFFECTS

To further investigate the inversion described in the main text, we compare results we find with the DEMNUni simulations to the smaller but highly resolved MassiveNuS simulations described in §2.

The main differences between the two simulations are their volume and resolution. Thus, comparing the void behavior in these simulations allows us to check if the inversion in the void abundance and power spectra is a volume and/or resolution artifact or physical in nature.

B1 Testing the effect of volume

Simulation volume can affect the number and size of voids: a simulation with an insufficiently large volume could miss large voids, and if the tracer density is held constant, reducing the simulation volume will decrease the number of voids found, eventually increasing the uncertainties so much that trends become indiscernible. It is therefore important to probe if the volumes of the simulations we use have an effect on our results.

In Figure B1 we plot the DEMNUni void-void power spectra after cutting the volume of the simulation to match that of the MassiveNuS simulation. We included voids with x, y, and z positions $0-512\,h^{-1}\mathrm{Mpc}$ of the origin and removed all others to produce the volume cut catalog.

Cutting the simulation volume maintains the overall shape of the void auto-correlation power spectrum. The elbow near $k \approx 10^{-1}\,h\mathrm{Mpc}^{-1}$ is still present, as is the rise to the left of the elbow. The scales probed by the volume cut simulation are smaller, so the power spectrum spans from only $k = 10^{-2}\,h\mathrm{Mpc}^{-1}$ to higher k for which the DEMNUni mass resolution becomes less reliable. For this reason, bins and uncertainties are larger for $k \lesssim 10^{-1}\,h\mathrm{Mpc}^{-1}$ in the volume cut simulation than in the original version.

Since increasing Σm_ν still boosts the overall power in the volume cut DEMNUni simulation, we conclude that the size of the DEMNUni and MassiveNuS simulations does not influence the inversion behavior we observe.

B2 Testing the effect of halo density

To probe how halo density affects the inversion, we randomly subsample the MassiveNuS simulation. We plot the void-void power spectra for different halo densities in Figure B2. Decreasing the halo density shifts the elbow towards large scales because the average void radius increases, and so the exclusion scale increases. Small scales increase in power due to the dependence of shot noise on tracer density (Hamaus et al. 2014a).

While decreasing the tracer density in the MassiveNuS simulation boosts the power, especially at small scales, it does not induce the Σm_ν inversion effect. This is in stark contrast to changing the minimum halo mass (see Figure B3), which induces an inversion effect as the threshold halo mass increases, increasing the halo bias, decreasing the total number of voids, and increasing the average void radius. This suggests physical characteristics of halos induce the inversion effect, justifying the paper's focus on halo bias.

APPENDIX C: MASSIVENUS VOID ABUNDANCE

In Figure C1 and Figure C2 we show the MassiveNuS abundances for the voids seen in the CDM field and the voids seen in the halo distribution, respectively. Uncertainties are

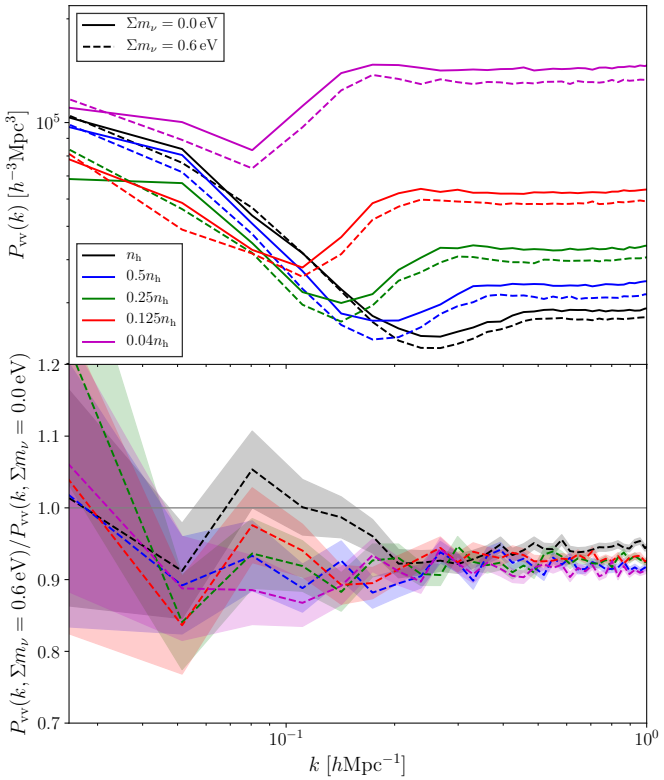


Figure B2. Void-void power spectra for the `MassiveNuS` simulations with different density cuts for voids traced by the halo distribution. Colors denote the tracer density cut of the simulation, where n_h is the original halo density. The tracer density $0.04n_\mathrm{h}$ corresponds to the halo density for the $M \geq 5\times10^{12}\,h^{-1}M_\odot$ mass threshold for the massless neutrino case. Dashed and solid lines denote the values of Σm_ν as described in the legend. The bottom panel shows the power spectra ratio with respect to the massless neutrino case, for each density cut simulation. The tracer density does not cause the inversion.

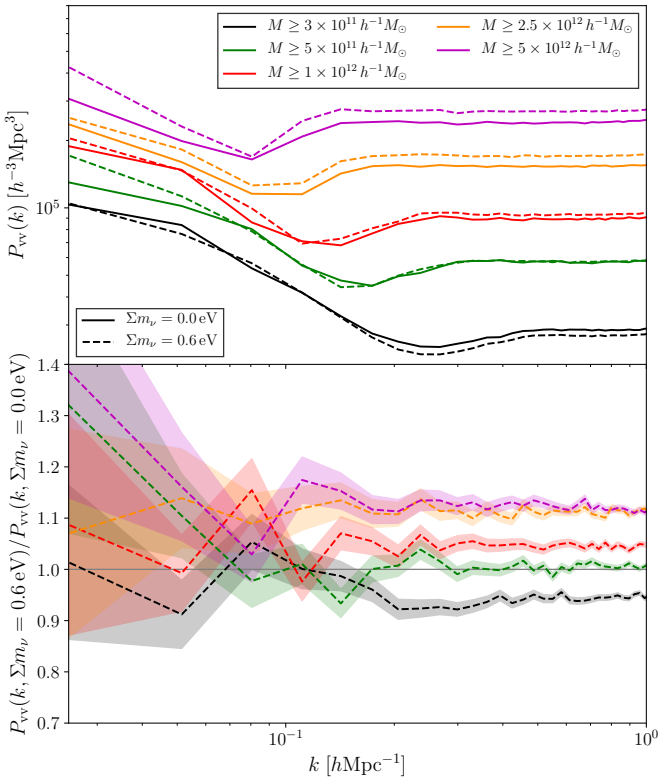


Figure B3. Void-void power spectra for the `MassiveNuS` simulations with different halo mass thresholds to illustrate the effects of halo bias. Colors denote the mass threshold of the simulation, where black is the original mass resolution. Dashed and solid lines denote the sum of neutrino masses used. The bottom panel shows the power spectra ratio between different Σm_ν for each halo mass threshold. As the mass threshold increases there is an inversion effect due to a larger halo bias and a smaller total number of voids.

large in Figure C2 due to the number of voids, making it difficult to definitively see clear trends for the different Σm_ν. However, for all Σm_ν, there are more small voids and less large voids relative to the massless case for voids seen in the halo field. Thus, it appears that abundances for voids seen in both the CDM field and the halo field are consistent with an increased number of small voids and decreased number of large voids as Σm_ν increases. This is in contrast to the `DEMNUni` abundance plots, which show clear opposite trends for the 2 tracer fields.

REFERENCES

Achitouv I., Cai Y.-C., 2018, preprint, (`arXiv:1806.04684`)

Achitouv I., Blake C., Carter P., Koda J., Beutler F., 2016, Physical Review D, 95

Ahmed S. N., et al., 2004, Physical Review Letters, 92, 181301

Alcock C., Paczyński B., 1979, Nature, 281, 358

Ali-Haïmoud Y., Bird S., 2013, Monthly Notices of the Royal Astronomical Society, 428, 3375

Alonso D., Hill J. C., Hložek R., Spergel D. N., 2018, Physical Review D, 97

Baldi M., Villaescusa-Navarro F., 2018, Monthly Notices of the Royal Astronomical Society, 473, 3226

Banerjee A., Dalal N., 2016, Journal of Cosmology and Astroparticle Physics, 2016

Barreira A., Cautun M., Li B., Baugh C. M., Pascoli S., 2015, Journal of Cosmology and Astroparticle Physics, 2015

Becker-Szendy R., et al., 1992, Phys. Rev. D, 46, 3720

Behroozi P. S., Wechsler R. H., Wu H. Y., 2013, Astrophysical Journal, 762

Biagetti M., Desjacques V., Kehagias A., Riotto A., 2014, Physical Review D - Particles, Fields, Gravitation and Cosmology, 90

Bond J. R., Kofman L., Pogosyan D., 1996, Nature, 380, 603

Bos E. G., van de Weygaert R., Dolag K., Pettorino V., 2012, Monthly Notices of the Royal Astronomical Society, 426, 440

Cai Y. C., Padilla N., Li B., 2014, Proceedings of the International Astronomical Union, 11, 555

Cai Y. C., Neyrinck M., Mao Q., Peacock J. A., Szapudi I., Berlind A. A., 2017, Monthly Notices of the Royal Astronomical Society, 466, 3364

Carbone C., Petkova M., Dolag K., 2016, Journal of Cosmology and Astroparticle Physics, 2016

Castorina E., Sefusatti E., Sheth R. K., Villaescusa-Navarro F., Viel M., 2014, Journal of Cosmology and Astroparticle Physics, 2014

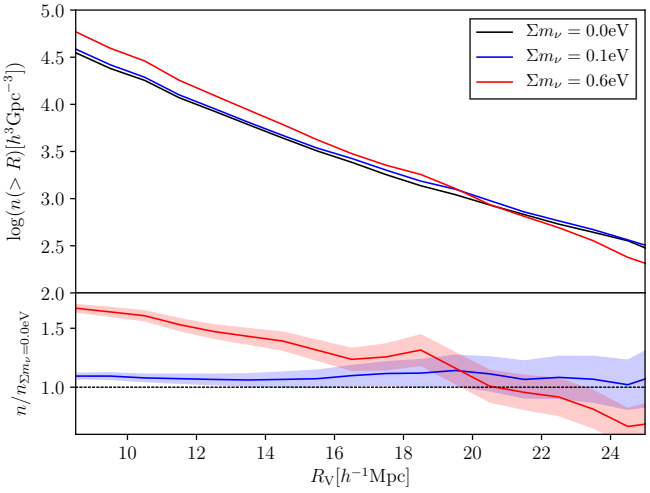


Figure C1. Void abundance in the CDM field of the `MassiveNuS` simulation. Colors denote the sum of neutrino masses used in each simulation. The bottom panel shows the ratio between void number density with uncertainties for the different Σm_ν values and the number density in the massless neutrino case. Increasing Σm_ν increases the number of small voids and decreases the number of large voids

.

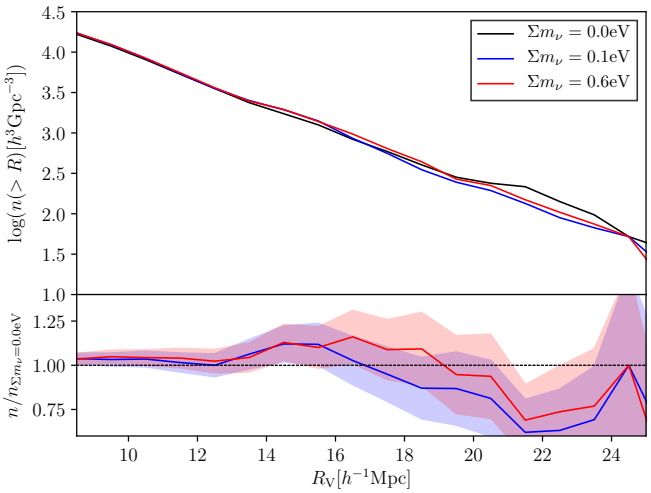


Figure C2. Void abundance in the halo field of the `MassiveNuS` simulation. Colors denote the sum of neutrino masses used in each simulation. The bottom panel shows the ratio between void number densities (with uncertainties) for different Σm_ν values and the number density in the massless neutrino case. Nonzero Σm_ν appears to increase the number of small voids and decrease the number of large voids relative to the massless case, in contrast to the `DEMNUni` abundance for voids traced by halos.

Castorina E., Carbone C., Bel J., Sefusatti E., Dolag K., 2015, Journal of Cosmology and Astroparticle Physics, 2015

Chan K. C., Hamaus N., Desjacques V., 2014, Physical Review D - Particles, Fields, Gravitation and Cosmology, 90

Chantavat T., Sawangwit U., Wandelt B. D., 2017, The Astrophysical Journal, 836

Clampitt J., Jain B., 2015, Monthly Notices of the Royal Astronomical Society, 454, 3357

Clampitt J., Cai Y. C., Li B., 2013, Monthly Notices of the Royal Astronomical Society, 431, 749

Clampitt J., et al., 2017, Monthly Notices of the Royal Astronomical Society, 465, 4204

Colberg J. M., et al., 2008, Monthly Notices of the Royal Astronomical Society, 387, 933

Davis M., Efstathiou G., Frenk C. S., White S. D. M., 1985, The Astrophysical Journal, 292, 371

De Bernardis F., Serra P., Cooray A., Melchiorri A., 2008, Physical Review D - Particles, Fields, Gravitation and Cosmology, 78

Desjacques V., Jeong D., Schmidt F., 2016, arXiv

Dolag K., Murante G., Borgani S., 2010, Monthly Notices of the Royal Astronomical Society, 405, 1544

Falck B., Neyrinck M. C., 2015, Monthly Notices of the Royal Astronomical Society, 450, 3239

Fukuda Y., et al., 1998, Physical Review Letters, 81, 1562

Gibbons G. W., Werner M. C., Yoshida N., Chon S., 2014, Monthly Notices of the Royal Astronomical Society, 438, 1603

Goldberg D. M., Vogeley M. S., 2004, The Astrophysical Journal, 605, 1

Granett B. R., Neyrinck M. C., Szapudi I., 2008, The Astrophysical Journal, 683, L99

Hamaus N., Wandelt B. D., Sutter P. M., Lavaux G., Warren M. S., 2014a, Physical Review Letters, 112

Hamaus N., Sutter P. M., Wandelt B. D., 2014b, Physical Review Letters, 112

Hamaus N., Sutter P. M., Lavaux G., Wandelt B. D., 2014c, Journal of Cosmology and Astroparticle Physics, 2014

Hamaus N., Sutter P. M., Lavaux G., Wandelt B. D., 2015, Journal of Cosmology and Astroparticle Physics, 2015

Hamaus N., Pisani A., Sutter P. M., Lavaux G., Escoffier S., Wandelt B. D., Weller J., 2016, Physical Review Letters, 117

Hamaus N., Cousinou M. C., Pisani A., Aubert M., Escoffier S., Weller J., 2017, Journal of Cosmology and Astroparticle Physics, 2017

Hawken A. J., et al., 2016, Astronomy & Astrophysics, 607

Ilić S., Langer M., Douspis M., 2013, Astronomy & Astrophysics, 556, A51

Kitaura F. S., et al., 2016, Physical Review Letters, 116

Kovács A., García-Bellido J., 2016, Monthly Notices of the Royal Astronomical Society, 462, 1882

Kovács A., Granett B. R., 2015, Monthly Notices of the Royal Astronomical Society, 452, 1295

Kovács A., et al., 2017, Monthly Notices of the Royal Astronomical Society, 465, 4166

Krolewski A., et al., 2017, A Detection of z˜2.3 Cosmic Voids from 3D Lyman-α Forest Tomography in the COSMOS Field (`arXiv:1710.02612`), `http://arxiv.org/abs/1710.02612`

Lavaux G., Wandelt B. D., 2012, Astrophysical Journal, 754

Lee J., Park D., 2009, Astrophysical Journal, 696

Lesgourgues J., Pastor S., 2006, Phys. Rep., 429, 307

Li B., Zhao G. B., Koyama K., 2012, Monthly Notices of the Royal Astronomical Society, 421, 3481

Liu J., Bird S., Matilla J. M. Z., Hill J. C., Haiman Z., Madhavacheril M. S., Spergel D. N., Petri A., 2018, Journal of Cosmology and Astroparticle Physics, 2018

Loverde M., 2014, Physical Review D - Particles, Fields, Gravitation and Cosmology, 90

Loverde M., 2016, Physical Review D, 93

Mao Q., Berlind A. A., Scherrer R. J., Neyrinck M. C., Scoccimarro R., Tinker J. L., McBride C. K., Schneider D. P., 2017, The Astrophysical Journal, 835, 160
Marulli F., Carbone C., Viel M., Moscardini L., Cimatti A., 2011, Monthly Notices of the Royal Astronomical Society, 418, 346
Massara E., Villaescusa-Navarro F., Viel M., 2014, Journal of Cosmology and Astroparticle Physics, 2014
Massara E., Villaescusa-Navarro F., Viel M., Sutter P. M., 2015, Journal of Cosmology and Astroparticle Physics, 2015
Melchior P., Sutter P. M., Sheldon E. S., Krause E., Wandelt B. D., 2013, Monthly Notices of the Royal Astronomical Society, 440, 2922
Nadathur S., Crittenden R., 2016, The Astrophysical Journal, 830, L19
Naidoo K., Benoit-Lévy A., Lahav O., 2016, Monthly Notices of the Royal Astronomical Society: Letters, 459, L71
Neyrinck M. C., 2008, Monthly Notices of the Royal Astronomical Society, 386, 2101
Odrzywołek A., 2009, Physical Review D - Particles, Fields, Gravitation and Cosmology, 80
Paranjape A., Lam T. Y., Sheth R. K., 2012, Monthly Notices of the Royal Astronomical Society, 420, 1648
Paz D., Lares M., Ceccarelli L., Padilla N., Lambas D. G., 2013, Monthly Notices of the Royal Astronomical Society, 436, 3480
Petracca F., Marulli F., Moscardini L., Cimatti A., Carbone C., Angulo R. E., 2016, Monthly Notices of the Royal Astronomical Society, 462, 4208
Pisani A., Sutter P., Lavaux G., Wandelt B., 2014, in Monthly Notices of the Royal Astronomical Society. pp 3238–3250 (arXiv:1306.3052), doi:10.1093/mnras/stu1399, https://academic.oup.com/mnras/article/443/4/3238/1018969
Pisani A., Sutter P. M., Hamaus N., Alizadeh E., Biswas R., Wandelt B. D., Hirata C. M., 2015, Physical Review D - Particles, Fields, Gravitation and Cosmology, 92
Planck Collaboration et al., 2013, Astronomy & Astrophysics, 571, A16
Planck Collaboration et al., 2018, preprint, (arXiv:1807.06209)
Pollina G., Baldi M., Marulli F., Moscardini L., 2016, Monthly Notices of the Royal Astronomical Society, 455, 3075
Pollina G., Hamaus N., Dolag K., Weller J., Baldi M., Moscardini L., 2017, Monthly Notices of the Royal Astronomical Society, 469, 787
Pollina G., et al., 2018, preprint, (arXiv:1806.06860)
Qin J., Liang Y., Zhao C., Yu H.-R., Liu Y., Zhang T.-J., 2017, arXiv
Raccanelli A., Verde L., Villaescusa-Navarro F., 2017, eprint arXiv:1704.07837
Ramachandra N. S., Shandarin S. F., 2017, Monthly Notices of the Royal Astronomical Society, 467, 1748
Ryden B., 1995, Astrophysical Journal, 452, 25
Shandarin S. F., 2011, Journal of Cosmology and Astroparticle Physics, 2011, 015
Springel V., Yoshida N., White S. D. M., 2001, New Astronomy, 6, 79
Sutter P. M., Lavaux G., Wandelt B. D., Weinberg D. H., 2012, Astrophysical Journal, 761
Sutter P. M., Lavaux G., Hamaus N., Wandelt B. D., Weinberg D. H., Warren M. S., 2014a, Mon. Not. R. Astron. Soc, 000, 0
Sutter P. M., Lavaux G., Wandelt B. D., Weinberg D. H., Warren M. S., 2014b, Monthly Notices of the Royal Astronomical Society, 438, 3177
Sutter P. M., Lavaux G., Wandelt B. D., Weinberg D. H., Warren M. S., Pisani A., 2014c, Monthly Notices of the Royal Astronomical Society, 442, 3127
Sutter P. M., Pisani A., Wandelt B. D., Weinberg D. H., 2014d, Monthly Notices of the Royal Astronomical Society, 443, 2983
Sutter P. M., Carlesi E., Wandelt B. D., Knebe A., 2014e, Monthly Notices of the Royal Astronomical Society: Letters, 446, L1
Sutter P. M., et al., 2015, Astronomy and Computing, 9, 1
Szapudi I., et al., 2015, Monthly Notices of the Royal Astronomical Society, 450, 288
Vagnozzi S., Brinckmann T., Archidiacono M., Freese K., Gerbino M., Lesgourgues J., Sprenger T., 2018, preprint, (arXiv:1807.04672)
Van De Weygaert R., Platen E., 2011, International Journal of Modern Physics: Conference Series, 01, 41
Viel M., Colberg J. M., Kim T. S., 2008, Monthly Notices of the Royal Astronomical Society, 386, 1285
Viel M., Haehnelt M. G., Springel V., 2010, Journal of Cosmology and Astroparticle Physics, 2010
Villaescusa-Navarro F., Vogelsberger M., Viel M., Loeb A., 2013, Monthly Notices of the Royal Astronomical Society, 431, 3670
Villaescusa-Navarro F., Marulli F., Viel M., Branchini E., Castorina E., Sefusatti E., Saito S., 2014, Journal of Cosmology and Astroparticle Physics, 2014
Zheng Z., et al., 2005, ApJ, 633, 791
Zivick P., Sutter P. M., 2014, Proceedings of the International Astronomical Union, 11, 589
de la Torre S., et al., 2013, A&A, 557, A54

This paper has been typeset from a TEX/LATEX file prepared by the author.